Flexible-Sector 6DMA Base Station: Modeling and Design

Yunli Li, *Member, IEEE*, Xiaoming Shi, Xiaodan Shao, *Member, IEEE*, Jie Xu, *Fellow, IEEE*, and Rui Zhang, *Fellow, IEEE*

***Abstract*—Six-dimensional movable antenna (6DMA) has emerged as a promising new technology for future wireless networks, which can adaptively adjust the three-dimensional (3D) positions and 3D rotations of antennas/antenna arrays for performance enhancement. This paper proposes a novel cost-effective 6DMA-based base station (BS) architecture, termed the *flexible-sector* BS, which allows the deployed antennas to flexibly rotate and move along a circular track, thus enabling common sector rotation and flexible antenna allocation across sectors to adapt to the spatial user distribution efficiently. In particular, we focus on the uplink transmission in a single-cell system, where the flexible-sector BS receives independent messages from multiple users. We introduce an angular-domain user distribution model, which captures the users' spatial clustering or hot-spot distribution effectively. Assuming the zero-forcing (ZF) based receiver applied at the BS to decode multiuser signals, we derive the average sum rate achievable for the users as a function of the common rotation of sectors and the antenna allocation over them. Moreover, we develop a two-step algorithm to jointly optimize the common sector rotation and antenna allocation to maximize the average sum rate of all users. It is shown that the optimal antenna number in each sector linearly increases with the number of users in it. It is also revealed that under the most favorable user distribution, the achievable sum rate gain increases in the order of $\log_2(B)$ in the regime of asymptotically large number of antennas, where B denotes the number of sectors. Numerically results also show that as B increases, the proposed flexible-sector BS achieves higher sum rate, and it outperforms other benchmark schemes, such as the traditional fixed-sector BS as well as the BS with sector rotation or antenna allocation optimization only.**

***Index Terms*—Flexible-sector base station, six-dimensional movable antenna (6DMA), angular-domain user distribution, zero-forcing (ZF) receiver, sector rotation, antenna allocation optimization.**

I. INTRODUCTION

Multiple-input multiple-output (MIMO) technology has played a pivotal role in wireless communication systems, which introduces new degrees of freedom (DoFs) in the spatial domain to enable significant array gains as well as spatial multiplexing and diversity gains, thereby substantially enhancing wireless communication rate and reliability [1]–[5]. Recently, wireless communication systems are increasingly shifting toward higher frequency bands such as millimeter-wave (mmWave) [6] and terahertz (THz) [7], with decreasing wavelength which allows for smaller-size antenna elements. This thus facilitates the deployment of MIMO systems at larger scales, and technologies such as massive MIMO [8]–[12] and extremely large-scale MIMO [13]–[18] have emerged. These systems leverage extensive antenna arrays to achieve higher array gains, compensate for the severe propagation losses, and more effectively suppress multi-user interference.

Despite such advancements, conventional MIMO systems primarily rely on fixed-antenna deployment at the base station (BS), where both antenna positions and coverage patterns remain static, even in the face of spatial and temporal fluctuations in wireless channels and user distributions. As such, these fixed-antenna BSs possess limited capability in dynamically adjusting beam directions, aperture configurations, and sector boundaries. This inflexibility results in inefficient spectrum usage in areas with low user density and network congestion in typical hotspots like stadiums and major transportation hubs. Consequently, fixed-antenna systems fail to fully exploit the spatial DoFs offered by MIMO, resulting in degraded spectral and energy efficiency, particularly under heterogeneous user distributions, rapidly changing mobility patterns, and highly dynamic channel conditions [19]–[22].

To tackle these issues, fluid antenna system (FAS) [23] and movable antenna (MA) [24] have been proposed as new techniques to enhance the antenna reconfiguration and adaptation capabilities, by dynamically adjusting antenna positions within a given physical aperture to adapt to the channel conditions. As such, they enable more efficient use of antenna DoFs as compared to traditional fixed-position antennas. However, FAS and MA techniques mainly exploit the small-scale channel fading to facilitate constructive/destructive combining of multipath signals, thereby enhancing desired signal strength and eliminating undesired interference for improving communication performance [25]–[28]. Thus, their practically achievable performance gains critically rely on the availability of accurate channel state information (CSI) and the sufficiently high movement speed of antennas to keep track of fast channel variation.

More recently, six-dimensional movable antenna (6DMA) has been proposed [29], which incorporates the new antenna

Y. Li and X. Shi are with the School of Science and Engineering, The Chinese University of Hong Kong, Shenzhen, Guangdong 518172, China (e-mail: yunlili@ieee.org, xiaomingshi@link.cuhk.edu.cn).

X. Shao is with Department of Electrical and Computer Engineering, University of Waterloo, Waterloo, ON N2L 3G1, Canada (e-mail: x6shao@uwaterloo.ca).

J. Xu is with the School of Science and Engineering (SSE), the Shenzhen Future Network of Intelligence Institute (FNii-Shenzhen), and the Guangdong Provincial Key Laboratory of Future Networks of Intelligence, The Chinese University of Hong Kong, Shenzhen, Guangdong 518172, China (e-mail: xujie@cuhk.edu.cn).

R. Zhang is with the Department of Electrical and Computer Engineering, National University of Singapore, Singapore 117583 (e-mail: elezhang@nus.edu.sg).

rotational DoF in addition to the antenna position adjustment of FAS/MA. This is achieved through the joint control of both three-dimensional (3D) positions and 3D rotations of antennas or antenna arrays. Notably, 6DMA has been shown to be able to leverage the knowledge of statistical CSI or user spatial distribution to adapt to large-scale channel variations and thereby enhance the multiuser communication rates [30]–[32]. Moreover, leveraging directional sparsity, channel estimation methods for arbitrary 6DMA positions and rotations were developed in [33]. Further advancing this architecture, a hierarchically-tunable 6DMA framework was proposed in [34], which pursues a sequential optimization of the arrays' global spherical positioning and individual local orientation tuning, thereby significantly reducing the computational complexity while improving the system performance. Additionally, a simplified implementation of 6DMA called circular 6DMA was proposed in [35], where distributed arrays at the BS can move along a circular track to adapt to the user distribution in the horizontal dimension.

It is also worth noting that existing fixed-antenna BSs widely adopt the sector antennas to achieve effective coverage with high directional gains, thus termed as sectorized BS [36]. Specifically, high-gain directional antennas are employed at the BS to divide its coverage area or cell into orthogonal sectors [37]. By concentrating radiated energy into narrow main lobes and suppressing sidelobes, such sector antennas achieve effective spatial isolation between adjacent sectors to suppress co-channel interference. This leads to improved signal-to-interference-plus-noise ratio (SINR), enables denser frequency reuse, and enhances the cell-edge throughput. However, traditional sectorized BSs still lack the capability of flexible antenna movement in terms of positioning and rotation like 6DMA; thus, it is appealing to upgrade sectorized BSs to 6DMA-enabled BSs for substantial throughput enhancement. Despite this promising potential, the state-of-the-art 6DMA designs [29]–[32], [34], [35], which are based on adjusting both 3D positions and 3D rotations of antenna arrays, are not compatible with existing sector antennas and sectorized BS architecture, thus requiring fundamental changes of the BS hardware and control mechanism. These challenges necessitate the development of a more cost-effective 6DMA BS design amenable to the existing sectorized BS architecture while preserving the high spatial adaptability and reconfigurability of 6DMA.

Motivated by the above, we propose a novel 6DMA-based BS architecture, termed the flexible-sector BS, in this paper. Fully compatible with the existing sectorized BSs, the directional antennas deployed at the flexible-sector BS to cover orthogonal sectors are capable of both rotating and moving along a circular track, thereby enabling dynamic sector rotation and flexible antenna allocation across sectors. This new adaptability allows the flexible-sector BS to respond to spatial variations in user distribution, thus significantly enhancing the system throughput yet with low movement overhead, hardware cost, and control complexity. The main results of this paper are outlined as follows.

- We propose an analytical and optimization framework for evaluating the performance of flexible-sector BS systems. Different from the existing studies on 6DMA-enabled BS [29]–[32], [34], [35], which rely on Monte-Carlo sampling for performance assessment through simulations, we present an analytical approach to characterize the system performance. To this end, we propose a new angular-domain user distribution model based on the two-dimensional (2D) finite homogeneous Poisson point process (FHPPP) to capture the users' spatial clustering or hot spot distribution in the angular domain. This model greatly facilitates the design of sector rotation and antenna allocation across sectors, while distinguishing from conventional distance-based stochastic models such as those built upon Poisson cluster process (PCP) and Matérn hard-core Poisson point process (PPP) [38]–[42].
- Under the angular-domain user distribution model, we consider the uplink transmission in a single-cell system, where multiple single-antenna users transmit independent messages to a multi-antenna flexible-sector BS. At each sector of the BS, we adopt the zero-forcing (ZF) based receiver together with channel-inversion-based power control for decoding the multiuser signals, ensuring that all users within the same sector achieve a common data rate. Within this framework, we further analyze the average sum rate achievable by all users in the cell served by the proposed flexible-sector BS as a function of the common sector rotation and cross-sector antenna allocation.
- Based on our analytical framework, we formulate an optimization problem aimed at maximizing the users' sum rate through the joint optimization of common sector rotation and antenna allocation across sectors. To solve this problem efficiently and extract useful insights, we develop a two-step algorithm. First, with any given common sector rotation, we derive a closed-form solution for the optimal antenna allocation. Then, the discrete common sector rotation is determined via one-dimensional search. Our results reveal that the optimal number of antennas allocated to each sector increases linearly with the number of users within the sector. Moreover, it is analytically shown that the flexible-sector BS achieves higher sum-rates when the average number of users varies more significantly across different sectors. In particular, when all users are clustered within a single sector by proper sector rotation, the proposed design achieves a per-user rate gain of $\log_2(B)$ in the regime of asymptotically large number of users with B denoting the number of sectors, compared to the conventional fixed-sector BS with equal user distribution over sectors.
- Finally, we present numerical results to validate the analysis under two representative user distributions, i.e., quasi-uniform and clustered random distributions, respectively. The results demonstrate that the proposed flexible-sector BS architecture with joint optimization of sector rotation and antenna allocation outperforms benchmark schemes that employ only one of these adaptation mechanisms. The performance improvement is more pronounced when users are more spatially clustered. Furthermore, the rate gain achieved by the flexible-sector BS becomes more substantial as the number of sectors increases, since

Table I: Summary of the main symbol notations used in this paper.

Notation	Description
$\mathcal{N}$, N	The set and number of antennas, respectively
$\mathcal{B}$, B	The set and number of sectors, respectively
Φ	The angular coverage span of each sector
$\mathcal{N}_b$, N_b	The set and number of antennas in sector b, respectively
d	The radius of the circular track at the BS
D	The radius of the cell
$A(\phi)$	The antenna gain in direction ϕ
$\mathcal{Z}$, Z	The set and number of zones, respectively
ψ	The angular range of each zone
$\mathcal{Z}_b$	The set of zones in sector b
c	The number of zones within each sector
z_0	The index of the first zone in $\mathcal{Z}_1$
λ_z	The user density of zone z
$\mathcal{K}_z$, K_z	The set and number of users in zone z, respectively
$\mathcal{Q}_b$, Q_b	The set and number of users in sector b, respectively
P_k	The transmit power of user k
$\boldsymbol{h}_k$, $\boldsymbol{g}_k$, ζ_k	The channel vector, small-scale fading vector, and average channel power gain from user k to the BS, respectively
$\boldsymbol{y}_b$, $\boldsymbol{H}_b$, ς_b	The received signal, combined channel matrix, and noise vector in sector b, respectively
$\boldsymbol{w}_k$	The ZF combining vector for user k
$\gamma_{b,k}$, $r_{b,k}$	The received SNR and ergodic rate of user k in sector b, respectively
R_b, R	The lower bounds of the sum rate of sector b and the overall system, respectively
$\boldsymbol{n}$	The antenna allocation vector over sectors
$\bar{r}$	The required minimum rate of users

more sectors provide higher antenna gains and greater flexibility in dynamic antenna allocation.

The rest of this paper is organized as follows. Section II presents the flexible-sector BS architecture, the angular-domain user distribution, and the resulting channel models. Section III characterizes the average rates achievable by users based on the ZF receiver. Section IV formulates the average sum-rate maximization problem. Section V presents a two-step algorithm for solving the formulated problem. Section VI investigates the effects of several key factors on the users' sum rate, including the required minimum rate of users, user distribution, and the number of sectors. Section VII reports numerical results under two representative user distributions, comparing the proposed flexible-sector BS against three benchmarks. Finally, Section VIII concludes this paper.

Notations: Scalars are denoted by lower-case letters, vectors by bold-face lower-case letters, and matrices by bold-face upper-case letters. $\boldsymbol{I}$ and $\boldsymbol{0}$ denote an identity matrix and an all-zero matrix, respectively, with appropriate dimensions. For a square matrix $\boldsymbol{S}$, $\boldsymbol{S}^{-1}$ denotes its inverse (if $\boldsymbol{S}$ is full-rank), and $[\boldsymbol{S}]_{k,k}$ denotes its k-th diagonal element. For a matrix $\boldsymbol{M}$ of arbitrary size, $\boldsymbol{M}^H$, $\boldsymbol{M}^T$, and $\mathbb{E}[\boldsymbol{M}]$ denote its conjugate transpose, transpose, and statistical expectation, respectively. The distribution of a circularly symmetric complex Gaussian (CSCG) random vector with mean $\mathbf{0}$ and covariance matrix $\boldsymbol{\Sigma}$ is denoted by $\mathcal{CN}(\mathbf{0}, \boldsymbol{\Sigma})$, and $\sim$ stands for "distributed as". $\mathbb{C}^{x\times y}$ denotes the space of $x \times y$ complex matrices. $\mathbb{C}$ denotes the set of complex numbers. $\mathbb{Z}_{++}$ denotes the set of positive integers. $\mathbb{Z}_{+}$ denotes the set of non-negative integers. $\mathbb{R}_{+}$ denotes the set of non-negative real numbers. $\|\boldsymbol{x}\|$ denotes the Euclidean norm of a complex vector $\boldsymbol{x}$. $|\cdot|$ denotes the cardinality of a set. $\overline{x}$ represents the mean value of a real number x. The operation $+$ is defined as $x^+ \triangleq \max\{x, 0\}$. $\binom{\cdot}{\cdot}$ denotes the binomial coefficient. Table I summarizes the main symbol notations used in this paper and their descriptions.

II. System Model

In this section, we first present the flexible-sector BS architecture. We then introduce the angular-domain user distribution model and the corresponding channel model.

A. Flexible-Sector BS

We consider the uplink transmission in a single-cell system consisting of a multi-antenna BS and multiple single-antenna users, as illustrated in Fig. 1(a). We assume that the BS is equipped with $N \geq 1$ antennas in total, denoted by set $\mathcal{N} \triangleq \{1, 2, \cdots, N\}$. The antennas are allocated to B sectors, denoted by set $\mathcal{B} \triangleq \{1, 2, \cdots, B\}$, with $B \geq 1$. Each sector is assumed to have an equal coverage in azimuth angle due to the use of directional antennas, which is given by angle $\Phi \triangleq \frac{2\pi}{B}$. Different from conventional BS with a fixed number of antennas in each sector, we propose a flexible-sector BS where the antennas at the BS can be flexibly allocated over different sectors. Specifically, the set of antennas in sector $b \in \mathcal{B}$ is denoted by set $\mathcal{N}_b, \mathcal{N}_b \subset \mathcal{N}$, with $N_b \triangleq |\mathcal{N}_b|$ denoting the number of antennas allocated to sector b. As shown in Fig. 1(a), the antennas are placed along a circular track with radius d at the BS, while those for each sector are placed at the angular center of each sector. The antennas can move freely along the circular track from one sector to another such that the number of antennas in each sector can be flexibly adjusted. Moreover, we assume that the angular centers of all antennas in different sectors can rotate flexibly along the circular track by a common azimuth angle, leading to corresponding rotations of orthogonal coverage regions of all sectors in azimuth angle. We set the center of the circular track as the reference position of the BS. The users are assumed to be randomly distributed on the ground within the circular cell of radius D and centered at the BS location.

To avoid interference across different sectors, we assume that the antennas in each sector have a directional radiation pattern (in the case of $B > 1$), which is modeled as a truncated function in azimuth angle.[1] Specifically, the azimuth

[1]When $B = 1$ and $\Phi = 2\pi$, the introduced system in Fig. 1 reduces to a single-sector BS with omnidirectional antennas.

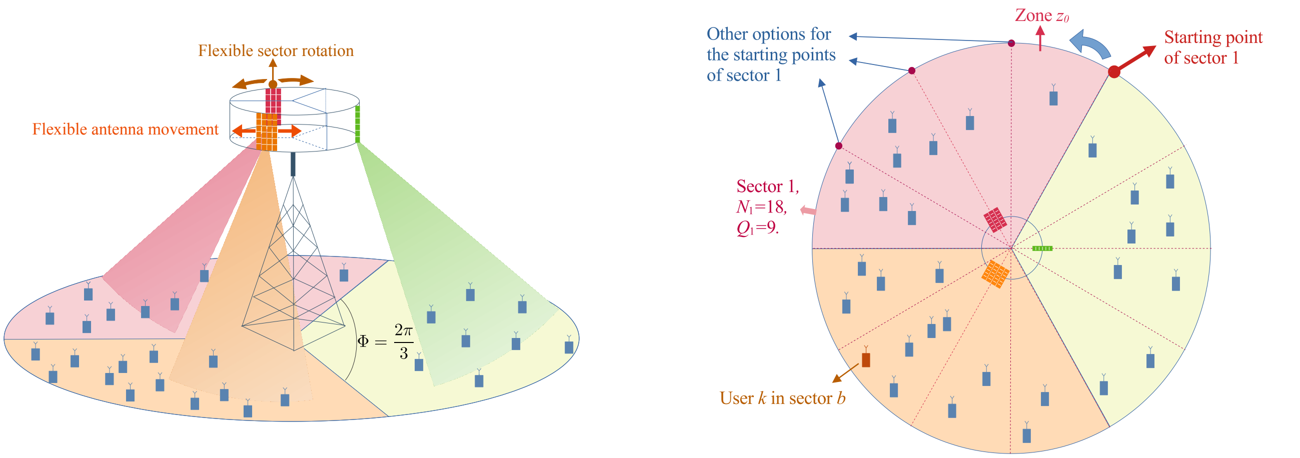

(a) Flexible-sector BS with $B = 3$ sectors.

(b) Angular zone-based user distribution with $c = 4$ zones in each sector.

Fig. 1. Illustration of the flexible-sector BS and angular zone-based user distribution.

beamwidth of each antenna is set to be Φ. Thus, the corresponding antenna gain in azimuth angle ϕ is given by [43], [44]

$$A(\phi) = \begin{cases} \frac{2\pi}{\Phi}, & -\frac{\Phi}{2} \leq \phi \leq \frac{\Phi}{2}, \\ 0, & \text{otherwise.} \end{cases} \tag{1}$$

Furthermore, we assume that each user is equipped with an omnidirectional antenna of unit gain.

To facilitate the joint design of antenna allocation among sectors and their common rotation, we propose an angular-domain approach to model the user distribution. As shown in Fig. 1(b), the whole cell is equally divided into Z zones in terms of azimuth angle, denoted by set $\mathcal{Z} \triangleq \{1, 2, \cdots, Z\}$ with $Z \geq 1$. For convenience, we assume $Z = cB$, where c is a positive integer. Accordingly, each sector $b \in \mathcal{B}$ consists of c zones, which are denoted by set $\mathcal{Z}_b$, expressed as

$$\mathcal{Z}_b = \{z_0 + (b-1)c, \cdots, z_0 + bc - 1\} \mod Z, \tag{2}$$

with $z_0 \in \{1, \cdots, c\}$ denoting the index of the first zone in $\mathcal{Z}_1$ (assuming that all the zones and sectors are arranged in a counter-clockwise manner). Thus, the common rotation of all sectors is controlled by adjusting z_0, which is referred to as the common rotation index, as shown in Fig. 1(b).

B. Angular-Domain User Distribution

We model the locations of users within each angular zone by the two-dimensional (2D) finite homogeneous Poisson point process (FHPPP)[2] [39], denoted by $\mathcal{K}_z$ with density λ_z, $\forall z \in \mathcal{Z}$. Thus, all users in the cell are denoted by set $\mathcal{K} = \bigcup_{z=1}^{Z} \mathcal{K}_z$. For analytical convenience, we assume that the number of users in each zone z is given, which corresponds to the average number of users derived from the user point process for that zone $z \in \mathcal{Z}$.

Let K_z and K denote the average number of users in zone z and that in the whole cell, respectively. Based on the FHPPP assumption, we have

$$K_z = \frac{1}{2}\psi D^2 \lambda_z, \quad z \in \mathcal{Z}, \tag{3}$$

and

$$K = \sum_{z=1}^{Z} K_z = \sum_{z=1}^{Z} \frac{1}{2}\psi D^2 \lambda_z, \tag{4}$$

where $\psi = \frac{2\pi}{Z}$ is the angular range of each zone.

We assume that each zone contains at least one user, i.e., $K_z \geq 1$, and $K < N$. Let $\mathcal{Q}_b(z_0) \triangleq \bigcup_{z \in \mathcal{Z}_b} \mathcal{K}_z$ denote the set of users located in sector b, $b \in \mathcal{B}$, and $Q_b(z_0)$ denote the average number of users in sector b, both of which depend on the corresponding zones of sector b that vary with the sectors' common rotation (i.e., z_0). Thus, $Q_b(z_0)$ is given by

$$Q_b(z_0) = \sum_{z \in \mathcal{Z}_b} K_z = \sum_{z=z_0+(b-1)c}^{z_0+bc-1} \frac{1}{2}\psi D^2 \lambda_z, \quad b \in \mathcal{B}. \tag{5}$$

For convenience, we assume in this paper that $Q_b(z_0) \geq 1, \forall b \in \mathcal{B}$, regardless of z_0, which is practically valid in general.

C. Channel Model

Last, we present the channel model between users and the BS. Based on the directional channel gain model in (1), the channel vector from user k in sector b to the BS is given by

$$\boldsymbol{h}_k = \sqrt{B\zeta_k}\boldsymbol{g}_k, \quad k \in \mathcal{Q}_b, \tag{6}$$

where B accounts for the directional antenna gain in each sector, ζ_k denotes the average channel power gain from user k to the reference point of the BS, and $\boldsymbol{g}_k \sim \mathcal{CN}(\boldsymbol{0}, \boldsymbol{I}_{N_b})$ denotes the complex channel vector characterizing the small-scale Rayleigh fading between user k and the antennas in sector b of BS, $\mathcal{N}_b$.

[2]In this work, we consider the channel inversion based power control to equalize the users' effective channel gains with the BS in each zone/sector, and as a result, our proposed design relies on the average number of users in each zone regardless of their locations in the zone. Nevertheless, the results obtained in this paper are also applicable to other (non-uniform) user distributions in each zone provided that the corresponding average numbers of users over angular zones are given.

The received signal at the BS in sector b is given by

$$\boldsymbol{y}_b = \sum_{k\in\mathcal{Q}_b} \boldsymbol{h}_k x_k + \boldsymbol{\varsigma}_b = \boldsymbol{H}_b \boldsymbol{x}_b + \boldsymbol{\varsigma}_b, \quad b\in\mathcal{B}, \tag{7}$$

where $x_k \in \mathbb{C}$ represents the transmitted information signal of user k with average power P_k, $\boldsymbol{H}_b = [\boldsymbol{h}_1, \cdots, \boldsymbol{h}_{Q_b}] \in \mathbb{C}^{N_b\times Q_b}$ represents the channel matrix from all users in $\mathcal{Q}_b$ to the BS's receive antennas in $\mathcal{N}_b$,[3] $\boldsymbol{x}_b = [x_1, \cdots, x_{Q_b}]^T \in \mathbb{C}^{Q_b\times 1}$, and $\boldsymbol{\varsigma}_b \sim \mathcal{CN}(\boldsymbol{0}, \delta^2 \boldsymbol{I}_{N_b})$ denotes the additive white Gaussian noise (AWGN) at the BS receiver, with δ^2 denoting the noise power. To achieve fair rate allocation among users, we consider the channel inversion power control at the users, such that the user transmit power is inversely proportional to the average channel power gain [45] with $P_k = \frac{P_0}{\zeta_k}$, where P_0 denotes the common power for all users in the cell. This ensures that the average received power is identical for users in the same sector.[4]

III. Average Achievable Rate

In this section, we first derive the achievable rate of user k in sector b, and then obtain the sum rate achievable for all users served by the BS. In order for ZF combining to be feasible, it is assumed that the number of antennas N_b in sector b is always no smaller than that of users Q_b, i.e., $N_b \geq Q_b$. We assume that the channel coefficients between all users and their serving antennas in each sector are perfectly known at the BS. The received signals from all users in sector b at its antennas are linearly combined, yielding

$$\widehat{\boldsymbol{x}}_b = \boldsymbol{W}_b^H \boldsymbol{y}_b, \quad b\in\mathcal{B}, \tag{8}$$

where $\boldsymbol{W}_b = [\boldsymbol{w}_1, \cdots, \boldsymbol{w}_{Q_b}]$, with $\boldsymbol{w}_k \in \mathbb{C}^{N_b\times 1}, k\in\mathcal{Q}_b$, denoting the combining vector for user k with $\|\boldsymbol{w}_k\| = 1$.

In this work, for simplicity we consider the ZF combining at each sector to perfectly eliminate the inter-user interference, i.e., $\boldsymbol{w}_k^H \boldsymbol{h}_j = 0, \forall j, k \in Q_b, j\neq k$. Specifically, we define

$$\overline{\boldsymbol{W}}_b = [\overline{\boldsymbol{w}}_1, \cdots, \overline{\boldsymbol{w}}_{Q_b}] = \boldsymbol{H}_b(\boldsymbol{H}_b^H \boldsymbol{H}_b)^{-1}, \quad b\in\mathcal{B}. \tag{9}$$

Thus, the ZF combining vector for user k is given by

$$\boldsymbol{w}_k = \frac{\overline{\boldsymbol{w}}_k}{\|\overline{\boldsymbol{w}}_k\|}, \quad k\in\mathcal{Q}_b. \tag{10}$$

Accordingly, the signal-to-noise ratio (SNR) for user k in sector b is given by [46]

$$\gamma_{b,k} = \frac{P_0}{\delta^2}|\boldsymbol{w}_k^H \boldsymbol{h}_k|^2 = \frac{P_0}{[(\boldsymbol{H}_b^H \boldsymbol{H}_b)^{-1}]_{k,k}\delta^2}, \quad k\in\mathcal{Q}_b. \tag{11}$$

The average achievable rate of user k in sector b is given by

$$r_{b,k} = \mathbb{E}\left[\log_2\left(1+\gamma_{b,k}\right)\right], \quad k\in\mathcal{Q}_b, \tag{12}$$

where the expectation is taken over the randomness of the small-scale Rayleigh fading channel coefficients.

Since the channel-inversion power control is applied within each sector, the average rates achievable for all users in the same sector are identical. Let $r_b, b\in\mathcal{B}$, denote the (identical) achievable rate of each user in sector b, with $r_b = r_{b,k}, \forall k\in\mathcal{Q}_b$. We have the following results to characterize the upper and lower bounds for rate r_b, denoted by $r_b^{(\mathrm{u})}$ and $r_b^{(\mathrm{l})}$, respectively.

[3]For notational convenience, we assume that the users in sector b are indexed from 1 to Q_b, and write $Q_b(z_0)$ as Q_b in short.

[4]There is no interference among sectors due to the use of directional antennas.

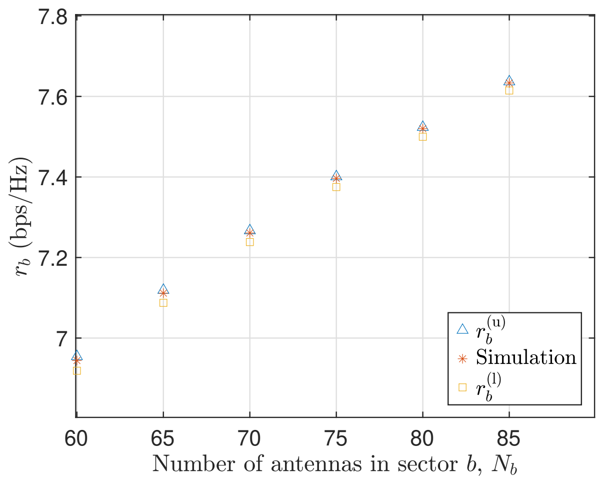

Fig. 2. Simulated user achievable rate versus the number of antennas in sector b.

Lemma 1. *The average achievable rate per user in sector b satisfies the following inequalities:*

$$r_b^{(\mathrm{l})} \leq r_b \leq r_b^{(\mathrm{u})}, \quad b\in\mathcal{B}, \tag{13}$$

where

$$r_b^{(\mathrm{u})} = \log_2\left(1+\frac{P_0\mathbb{E}\left[|\boldsymbol{w}_k^H\boldsymbol{h}_k|^2\right]}{\delta^2}\right), \quad k\in\mathcal{Q}_b, \tag{14}$$

and

$$r_b^{(\mathrm{l})} = \log_2\left(1+\frac{P_0}{\mathbb{E}\left[[(\boldsymbol{H}_b^H\boldsymbol{H}_b)^{-1}]_{k,k}\right]\delta^2}\right), \quad k\in\mathcal{Q}_b. \tag{15}$$

More specifically, $r_b^{(\mathrm{u})}$ in (14) *can be expressed as a function of the common rotation index, z_0, and the number of antennas allocated to sector b, N_b, which is given by*

$$r_b^{(\mathrm{u})}(N_b, z_0) = \log_2\left[1+B\gamma_0(N_b - Q_b(z_0)+1)^+\right], \quad b\in\mathcal{B}, \tag{16}$$

where $\gamma_0 = \frac{P_0}{\delta^2}$; and $r_b^{(\mathrm{l})}$ in (15) *can be expressed as*

$$r_b^{(\mathrm{l})}(N_b, z_0) = \log_2\left[1+B\gamma_0(N_b - Q_b(z_0))^+\right], \quad b\in\mathcal{B}. \tag{17}$$

Proof: See Appendix A. □

From Lemma 1, it follows that the upper and lower bounds for the achievable rate of users in sector b, given in (16) and (17) respectively, are explicitly expressed in terms of the numbers of antennas and users in the sector. Moreover, it is observed from Fig. 2 that these bounds are generally very tight. As such, we adopt the lower bound as the average achievable rate per user for sector b for system design and optimization in the rest of this paper. Accordingly, the lower bound of the sum rate of all users in sector b is given by

$$R_b(N_b, z_0) \triangleq Q_b(z_0) r_b^{(1)}(N_b, z_0), \quad b \in \mathcal{B}. \tag{18}$$

Finally, the lower bound of the sum rate of all users in all sectors of the cell is given by

$$\begin{aligned} R(\boldsymbol{n}, z_0) &= \sum_{b=1}^{B} R_b(N_b, z_0) \\ &= \sum_{b=1}^{B} Q_b(z_0) \log_2\left[1 + B\gamma_0 (N_b - Q_b(z_0))^+\right], \end{aligned} \tag{19}$$

where $\boldsymbol{n} = [N_1, \cdots, N_B]^T \in \mathbb{Z}_+^B$ denotes the collective vector indicating the number of antennas allocated to each sector.

IV. Problem Formulation

In this paper, we aim to maximize the sum rate of all users served by the flexible-sector BS through the joint optimization of the antenna allocation $\boldsymbol{n}$ over sectors and the common rotation index z_0 of sectors. In the following, we use the lower bound given in (19) to represent the sum-rate of all users for convenience. The sum-rate maximization problem is thus formulated as

$$\text{(P1)}: \quad \max_{\boldsymbol{n} \in \mathbb{Z}_+^B, z_0 \in \mathbb{Z}_{++}} \quad R(\boldsymbol{n}, z_0)$$

$$\text{s.t.} \quad \sum_{b=1}^{B} N_b \le N, \tag{20a}$$

$$r_b^{(l)}(N_b, z_0) \ge \overline{r}, \forall b \in \mathcal{B}, \tag{20b}$$

$$1 \le z_0 \le c, \tag{20c}$$

where (20a) denotes the total antenna budget at the BS, and (20b) represents the minimum rate constraints for all users with $\overline{r} > 0$ denoting the minimum rate required for all users. (P1) is an integer programming problem and can be optimally solved by the exhaustive search over $\boldsymbol{n}$ and z_0 in their joint discrete set. However, this approach is computationally prohibitive (with complexity in the order of $O\left(c\binom{N-1}{B-1}\right)$) when N and/or B is large, and also fails to reveal any useful insights into the optimal solution. Thus, in this paper, we propose an alternative approach to solve (P1), by relaxing the discrete variables $N_b, \forall b \in \mathcal{B}$, into continuous ones, as detailed in Section V.

Before we proceed to solve (P1), we note that to ensure the feasibility of problem (P1), from (17) and (20b) the following constraints need to be satisfied:

$$N_b \ge Q_b(z_0) + \frac{2^{\overline{r}} - 1}{B\gamma_0} \triangleq N_{b,\min}, \quad \forall b \in \mathcal{B}, \tag{21}$$

which, together with the constraint (20a) and the fact that $\sum_{b=1}^{B} Q_b(z_0) = K$, leads to the following constraint over $\overline{r}$:

$$\overline{r} \le \log_2\left[1 + \gamma_0(N - K)\right] \triangleq \overline{r}_{\max}. \tag{22}$$

In the sequel of this paper, we replace the constraint (20b) of (P1) with its equivalent one in (21).

V. Proposed Solution to Problem (P1)

Since the feasible set of the common rotation of sectors z_0 consists of a finite number of discrete values, we address problem (P1) by adopting a two-step approach. First, we determine the antenna allocation policy for $\boldsymbol{n}$ with any given z_0. Then, we perform a discrete search over the feasible set of z_0 to determine the overall solution to (P1).

A. Antenna Allocation Optimization with Given Common Sector Rotation

With given common rotation index z_0, the optimization of antenna allocation $\boldsymbol{n}$ in problem (P1) is simplified as

$$\text{(P2)}: \quad \max_{\boldsymbol{n} \in \mathbb{Z}_+^B} \quad \sum_{b=1}^{B} Q_b \log_2\left[1 + B\gamma_0(N_b - Q_b)\right]$$

$$\text{s.t.} \quad \sum_{b=1}^{B} N_b \le N, \tag{23a}$$

$$N_b \ge Q_b + \frac{2^{\overline{r}} - 1}{B\gamma_0}, \quad \forall b \in \mathcal{B}. \tag{23b}$$

Note that in the objective function of (P2) we omit z_0 in $Q_b(z_0)$ since z_0 is fixed. In addition, we have removed the '$+$' operation in the objective function of (P2) due to constraint (23b).

Next, we relax $N_b, \forall b \in \mathcal{B}$, to continuous variables. Thus, problem (P2) is reformulated as

$$\text{(P3)}: \quad \max_{\boldsymbol{n} \in \mathbb{R}_+^B} \quad \sum_{b=1}^{B} Q_b \log_2\left[1 + B\gamma_0(N_b - Q_b)\right]$$

$$\text{s.t.} \quad \sum_{b=1}^{B} N_b \le N, \tag{24a}$$

$$N_b \ge N_{b,\min}, \quad \forall b \in \mathcal{B}. \tag{24b}$$

Thus, problem (P2) is transformed from a non-convex integer program to a convex optimization problem over continuous N_b's.

It can be verified that problem (P3) is a convex optimization problem, since the objective function is concave and the constraints are linear.

Proposition 1. *The optimal semi-closed-form solution to* (P3) *is given by*

$$N_b^\star = \max\left\{Q_b\left(1 + \frac{1}{\nu \ln 2}\right) - \frac{1}{B\gamma_0}, N_{b,\min}\right\}, \quad b \in \mathcal{B}, \tag{25}$$

where ν is a unique constant that satisfies the following equation:

$$\sum_{b=1}^{B} \max\left\{Q_b\left(1 + \frac{1}{\nu \ln 2}\right) - \frac{1}{B\gamma_0}, N_{b,\min}\right\} = N. \tag{26}$$

Proof: See Appendix B. □

The value of ν can be numerically found by a simple bisection search based on (26). From (21) and (25), it is worth noting that $N_b^\star$ is a monotonically increasing function of Q_b, which is intuitively expected since more antennas need

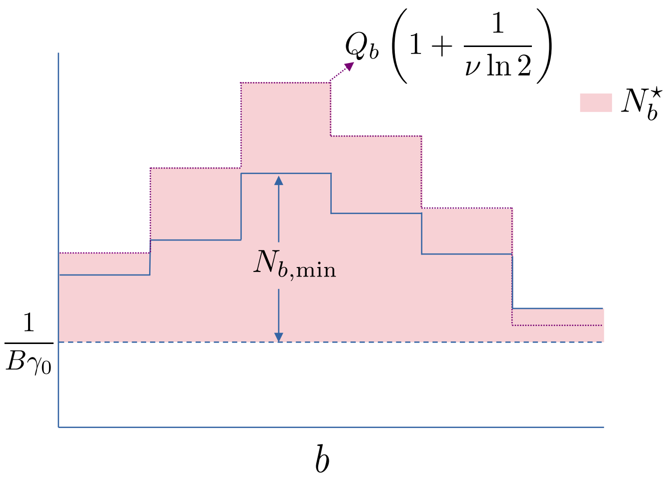

Fig. 3. Illustration of the solution given in (25).

Algorithm 1 Proposed solution for problem (P1)

Given $\bar{r} \le \bar{r}_{\max}$.
for $z_0 = 1 : c$ **do**
  Calculate $Q_b(z_0), \forall b \in \mathcal{B}$, using (5);
  Calculate $N_b^\star(z_0), \forall b \in \mathcal{B}$, using (25), (26) and (27);
  Calculate $R(z_0)$ using (28);
end for
$z_0^\star = \arg_{z_0 \in \{1,\cdots,c\}} \max R(z_0)$.
$\boldsymbol{n}^\star(z_0^\star) = \{N_1^\star(z_0^\star), \cdots, N_B^\star(z_0^\star)\}$.
Return $z_0^\star, \boldsymbol{n}^\star(z_0^\star)$.

to be allocated to sector b when there are more users in it for achieving higher rates. An illustration for $N_b^\star$ given in (25) is provided in Fig. 3.

Next, based on the relaxed solution in Proposition 1 for (P3), we obtain the solution of (P2) by mapping the solution derived in (25) back to the original discrete space. This can be achieved by rounding the solution in (25) to the nearest integer no greater than it, i.e.,

$$N_b^\star(z_0) \leftarrow \lfloor N_b^\star \rfloor, \quad \forall b \in \mathcal{B}. \tag{27}$$

B. Optimization of Common Rotation Index

By substituting $N_b^\star(z_0)$ given in (27) into the objective function of problem (P1), we obtain the users' maximum sum rate with given z_0 as

$$R(z_0) = \sum_{b=1}^{B} Q_b(z_0) \log_2 \left\{1 + B\gamma_0[N_b{}^\star(z_0) - Q_b(z_0)]\right\}. \tag{28}$$

Then, the optimal z_0 can be found by a simple exhaustive search over $z_0 \in \{1, \cdots, c\}$, denoted by $z_0^\star$. As a result, the corresponding solutions of N_b's for (P1) are obtained as $N_b^\star(z_0^\star), b \in \mathcal{B}$. The above procedure for solving problem (P1) is summarized in Algorithm 1.

VI. Effects of Key Factors on Users' Sum Rate

In this section, we use the solution obtained by solving problem (P1) to analyze the effects of several key system factors on the users' maximum sum rate given in (28), including the required minimum rate of users $\bar{r}$, the user distribution in terms of the numbers of users in different sectors, i.e., $Q_b, b \in \mathcal{B}$, and the number of sectors B. Note that we omit z_0 in the terms involving it in (28) in this section, since the derived results apply for any given z_0, including the optimal $z_0^\star$ for problem (P1). In addition, we assume continuous antenna allocation over sectors for ease of analysis.

A. Minimum Rate of Users

In this subsection, we study the impact of the required minimum rate of users $\bar{r}$ on the solution of problem (P1) and the resulting users' maximum sum rate.

From (25), it follows that, if the following conditions are satisfied:

$$Q_b\left(1+\frac{1}{\nu \ln 2}\right) - \frac{1}{B\gamma_0} \ge N_{b,\min}, \quad \forall b \in \mathcal{B}, \tag{29}$$

we obtain

$$N_b^\star = Q_b\left(1+\frac{1}{\nu \ln 2}\right) - \frac{1}{B\gamma_0}, \quad b \in \mathcal{B}. \tag{30}$$

Moreover, from (26) and under the same conditions in (29), we derive a closed-form expression for ν as

$$\nu = \frac{K}{\left(N - K + \frac{1}{\gamma_0}\right)\ln 2}. \tag{31}$$

By substituting ν in (31) into (30), we obtain

$$N_b^\star = \frac{Q_b}{K}\left(N + \frac{1}{\gamma_0}\right) - \frac{1}{B\gamma_0}, \quad b \in \mathcal{B}. \tag{32}$$

Note that (32) holds if and only if $N_{b,\min} \le N_b^\star$ for all b's. Thus, from (21), we can show

$$\bar{r} \le \log_2\left(\frac{BQ_b[(N-K)\gamma_0 + 1]}{K}\right), \quad \forall b \in \mathcal{B}, \tag{33}$$

which can be equivalently written as

$$\bar{r} \le \log_2\left(\frac{BQ_{b,\min}[(N-K)\gamma_0 + 1]}{K}\right) \triangleq \bar{r}_0. \tag{34}$$

Accordingly, when $\bar{r} \le \bar{r}_0$, the users' maximum sum rate in (28) is given by

$$R = \sum_{b=1}^{B} Q_b \log_2\left[B\gamma_0 \frac{Q_b}{K}\left(N - K + \frac{1}{\gamma_0}\right)\right]. \tag{35}$$

To draw more useful insights, in the rest of this section, we assume that $\bar{r}$ is sufficiently small such that $\bar{r} \le \bar{r}_0$ holds, which is usually the case in practice (e.g., massive MIMO systems) with $N \gg K$, and thus the antenna allocation and sum rate of users are given in closed form in (32) and (35), respectively.

B. User Distribution

To characterize the effect of user distribution or equivalently the numbers of users over sectors, Q_b's, on the users' maximum sum rate in (35), we formulate a new optimization problem to maximize the sum rate given in (35) by assuming that Q_b's can be freely allocated over sectors subject to the given total number of users, K. Note that we assume that the antenna allocation is optimal for any given Q_b's as given in (32). For analytical convenience, we relax $Q_b, \forall b \in \mathcal{B}$, to continuous values, and thus the problem is formulated as[5]

$$\text{(P4)}: \quad \max_{\boldsymbol{q}\in\mathbb{R}_+^B} \quad \sum_{b=1}^{B} Q_b \log_2\left[\frac{Q_b B\gamma_0}{K}\left(N-K+\frac{1}{\gamma_0}\right)\right]$$

$$\text{s.t.} \quad \sum_{b=1}^{B} Q_b = K, \tag{36a}$$

$$Q_b \geq 1, \forall b \in \mathcal{B}, \tag{36b}$$

where $\boldsymbol{q} \triangleq [Q_1, \cdots, Q_B]^T \in \mathbb{R}_+^B$ denotes the collective vector indicating the number of users in each sector, and (36b) is required for the condition (20b) in problem (P1) to be valid.

The objective function in problem (P4) is a convex function. Thus, problem (P4) is a non-convex optimization problem and difficult to solve in general. However, by exploiting the special structure of (P4), i.e., the objective function consists of identical terms in terms of Q_b's, the optimal solution for problem (P4) can be derived, which is given by

$$\begin{cases} Q_i^\star = & K-B+1, \quad \exists i \in \mathcal{B}, \\ Q_j^\star = & 1, \quad \forall j \neq i, j \in \mathcal{B}. \end{cases} \tag{37}$$

Thus, the corresponding antenna allocation is given by

$$\begin{cases} N_i^\star = & \frac{K-B+1}{K}\left(N+\frac{1}{\gamma_0}\right)-\frac{1}{B\gamma_0}, \\ N_j^\star = & \frac{N-N_i^\star}{B-1}, \quad \forall j \neq i, j \in \mathcal{B}. \end{cases} \tag{38}$$

From (37) and (38), we observe that it is optimal to have users located in one sector only as much as possible, and so is the number of antennas allocated to this sector. In practical scenarios, condition (36b) can be safely omitted since its main purpose is to ensure the feasibility of problem (P4) from a mathematical standpoint. Thus, we define the most favorable user distribution for attaining the maximum sum rate with the flexible-sector BS as

$$\begin{cases} Q_i = K, & \exists i \in \mathcal{B}, \\ Q_j = 0, & \forall j \neq i, j \in \mathcal{B}. \end{cases} \tag{39}$$

With the optimal user distribution given in (39), the corresponding optimal antenna allocation is given by

$$\begin{cases} N_i = N, & \\ N_j = 0, & \forall j \neq i, j \in \mathcal{B}, \end{cases} \tag{40}$$

and from (19) the resulting maximum sum rate of all users is given by

$$R_{\max} = K\log_2\left[1+B\gamma_0(N-K)\right]. \tag{41}$$

[5]In (35), the required minimum rate for all users is guaranteed, and thus there is no constraint on the minimum rate of users in problem (P4).

Moreover, to obtain more insights, we formulate a problem to minimize the sum rate of all users (instead of maximizing it in (P4)), which is given by

$$\text{(P5)}: \quad \min_{\boldsymbol{q}\in\mathbb{R}_+^B} \quad \sum_{b=1}^{B} Q_b \log_2\left[\frac{Q_b B\gamma_0}{K}\left(N-K+\frac{1}{\gamma_0}\right)\right]$$

$$\text{s.t.} \quad \sum_{b=1}^{B} Q_b = K, \tag{42a}$$

$$Q_b \geq 1, \forall b \in \mathcal{B}. \tag{42b}$$

Since the objective function in problem (P5) is convex and the constraints are linear, (P5) is a convex optimization problem. By applying the Jensen's inequality, we can easily show that in (P5), the minimum sum rate of all users is attained when the users are equally distributed among all sectors, leading to (assuming $K \geq B$)

$$Q_b^\star = \frac{K}{B}, \quad \forall b \in \mathcal{B}. \tag{43}$$

The corresponding antenna allocation is given by

$$N_b^\star = \frac{N}{B}, \quad b \in \mathcal{B}, \tag{44}$$

and the resulting users' minimum sum rate is given by

$$\begin{aligned} R_{\min} &= K\log_2\left[1+B\gamma_0\left(\frac{N}{B}-\frac{K}{B}\right)\right], \\ &= K\log_2\left[1+\gamma_0(N-K)\right], \end{aligned} \tag{45}$$

which is smaller than or equal to $R_{\max}$ in (41), while the equality holds when $B=1$.

Comparing (41) and (45), we reveal that the minimum sum rate of all users occurs when users are uniformly distributed across all sectors according to (43), whereas the maximum sum rate of all users is achieved when users are distributed according to (39), i.e., all users are located in one sector with no users located in any other sectors (termed as the most favorable user distribution for flexible-sector BS). Thus, it can be inferred that the common rotation of sectors, i.e., $z_0^\star$, in problem (P1), should be set to result in unevenly/sparsely distributed users over sectors as much as possible (in the ideal case, approaching to that given in (39)), so as to maximize the users' sum rate. Moreover, in problem (P1), the sum rate of all users is upper-bounded by $R_{\max}$ given in (41) and lower-bounded by $R_{\min}$ given in (45), regardless of the user spatial distributions over angular zones.

Theorem 1. *From* (41) *and* (45)*, the asymptotic rate gain, defined as the gap between the maximum and minimum achievable rates per user, with the flexible-sector BS under the most favorable user distribution in* (39) *when N goes to infinity (i.e., $N \gg B$) is given by*

$$\frac{R_{\max}}{K} - \frac{R_{\min}}{K} = \log_2 B, \tag{46}$$

in bits-per-second-per-Hertz (bps/Hz).

The rate gain given in Theorem 1 is explained as follows. When the users are distributed according to (39) within one sector only, the flexible-sector BS can allocate all the antennas to cover this sector by properly setting the sector rotation and moving all antennas from the other sectors to this sector. This results in a sector array gain after applying the ZF combining, which is equal to $(N-K)$ shown in (41). In contrast, when the users are equally distributed over a set of B sectors given in (43), the flexible-sector BS just needs to properly set its sector rotation (if needed) to cover these sectors, while the antennas are equally allocated to all sectors (similar to the conventional fixed-sector BS with equal antenna allocation over sectors serving users evenly distributed over sectors). This, however, results in a reduced array gain after ZF combining, which is equal to $(N/B-K/B) = (N-K)/B$ given in (45). Thus, the rate gain of the flexible-sector BS over the conventional fixed-sector BS critically depends on the user spatial distribution.

C. Number of Sectors

Finally, we analyze the impact of B on the users' maximum sum rate by considering non-uniformly distributed users in this subsection. We consider two scenarios under the same user distribution with identical sector rotation z_0 of the flexible-sector BS to investigate the system performance under different setups of B.

- **Scenario I**: There are B_0 sectors. Let $Q_b^{(\mathrm{I})}$ denote the number of users in sector $b, b \in \{1, \cdots, B_0\}$, for the given sector rotation z_0. From (35), the users' sum rate with optimal antenna allocation is given by

$$R^{(\mathrm{I})} = \sum_{b=1}^{B_0} Q_b^{(\mathrm{I})} \log_2 \left[B\gamma_0 \frac{Q_b^{(\mathrm{I})}}{K} \left(N - K + \frac{1}{\gamma_0} \right) \right]. \tag{47}$$

- **Scenario II**: There are $2B_0$ sectors. Let $Q_b^{(\mathrm{II})}$ denote the number of users in sector $b, b \in \{1, \cdots, 2B_0\}$. Based on (35), the users' sum rate is given by

$$R^{(\mathrm{II})} = \sum_{b=1}^{2B_0} Q_b^{(\mathrm{II})} \log_2 \left[2B_0\gamma_0 \frac{Q_b^{(\mathrm{II})}}{K} \left(N - K + \frac{1}{\gamma_0} \right) \right]. \tag{48}$$

Note that the sector rotation z_0 in Scenario II satisfies that for any $j = 2i-1, i \in \{1, \cdots, B_0\}$, $Q_j^{(\mathrm{II})} + Q_{j+1}^{(\mathrm{II})} = Q_i^{(\mathrm{I})}, \forall i, j$. Then, from (47) and (48), it follows that

- If $Q_j^{(\mathrm{II})} = Q_{j+1}^{(\mathrm{II})}, \forall i, j$, $R^{(\mathrm{I})} = R^{(\mathrm{II})}$.
- Otherwise, if there exists i, j, such that $Q_j^{(\mathrm{II})} \neq Q_{j+1}^{(\mathrm{II})}$, then $R^{(\mathrm{I})} < R^{(\mathrm{II})}$, which can be shown similarly as the solution of problem (P4).

Remark 1: Based on the above results, it is evident that if the users are non-uniformly distributed, a larger number of sectors generally tend to enhance the sum rate of users. This is expected since both higher directional antenna gain and higher flexibility in antenna allocation over sectors are offered. This enhancement, however, is accompanied by an increase in hardware cost and implementation complexity.

VII. Numerical Results

In this section, we provide numerical results to validate the effectiveness of the proposed flexible-sector BS design by evaluating its performance under two distinct user distribution scenarios. These scenarios are designed to showcase the adaptability and advantages of the optimized antenna allocation strategy, denoted as $N_b^{\star}, b \in \mathcal{B}$, which was derived in Section V. The following parameters are considered unless specified otherwise. The radius of the cell is $D = 100$ m, the total number of antennas is $N = 90$, the number of users is $K = 50$, the deployment area is divided into $Z = 30$ zones, the start point of zone 1 is at 0°, the normalized SNR is set to $\gamma_0 = 0$ dB, and the minimum user rate requirement is $\bar{r} = 5$ bps/Hz.

We consider the following two distinct user distribution scenarios, as depicted in Figs. 4 and 5, respectively. For each scenario, both the spatial realizations and the corresponding angular domain representations of user locations are presented.

- User distribution-I (Quasi-uniform distribution): The whole cell is partitioned into 2 angular regions, within each of which users are uniformly distributed, as illustrated in Fig. 4. For example, for zones $16-25$, the average number of users in each zone is 3 while that for the other zones is 1. Consequently, under any given B considered in our simulations, we can find a proper value of z_0, such that the numbers of users in different sectors are identical.
- User distribution-II (Clustered random distribution): The whole cell is also partitioned into 2 angular regions. Most users are concentrated within a narrow angular span (i.e., zones 16–25), with only a few scattered across the remaining zones, as shown in Fig. 5. As the sector boundaries rotate, this dense user cluster shifts from one sector to another, causing large fluctuations in the number of users per sector.

These two user distributions are designed to model scenarios featuring angularly uniform hotspots as well as non-uniform angular user concentrations. The resulting insights obtained from these distributions are readily extendable to scenarios involving arbitrary combinations of uniform and non-uniform user clusters in the angular domain.

Figs. 6(a) and 6(b) show the average sum rate of all users versus the common rotation index z_0 for user distributions I and II, respectively, with different values of the number of sectors B. The periodic behavior of the curves indicates that we only need to consider $z_0 \in \{1, \cdots, B/Z\}$, as other values of z_0 will lead to the repeated result. It is observed that the sum rate of all users for both two user distribution scenarios is maximized when the number of sectors B is set to its upper limit in our setup. This empirical finding is consistent with the theoretical insights given in Remark 1, as a larger sector number B provides higher directional antenna gains and greater control flexibility for the proposed flexible-sector BS. Next, for user distribution-I, it is observed from Fig. 6(a) that the same maximum sum rate is achieved for any value of $B > 1$. Although for $B = 30$ any value of z_0 leads to the same maximum sum rate, for $B < 30$ properly selecting

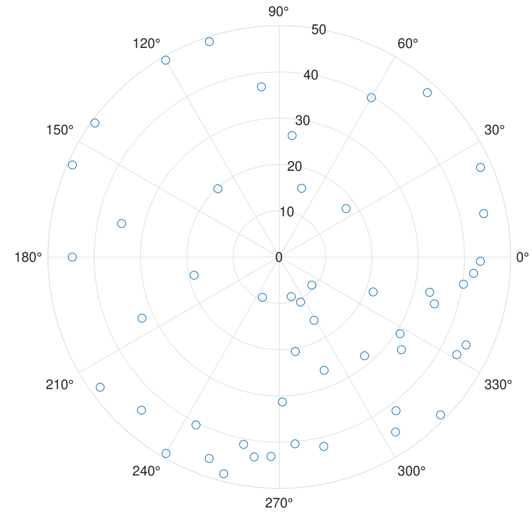

(a) Polar illustration.

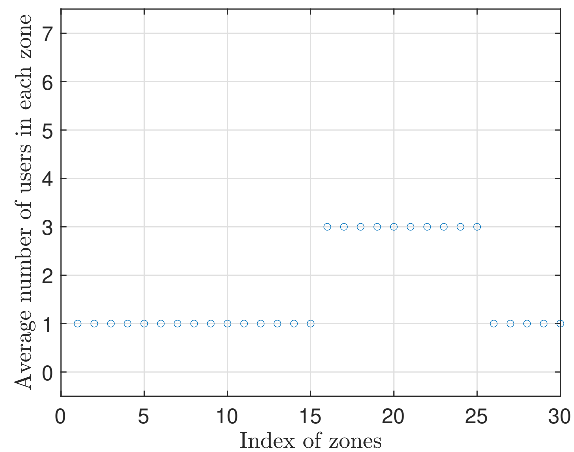

(b) Angular-domain illustration.

Fig. 4. User distribution-I.

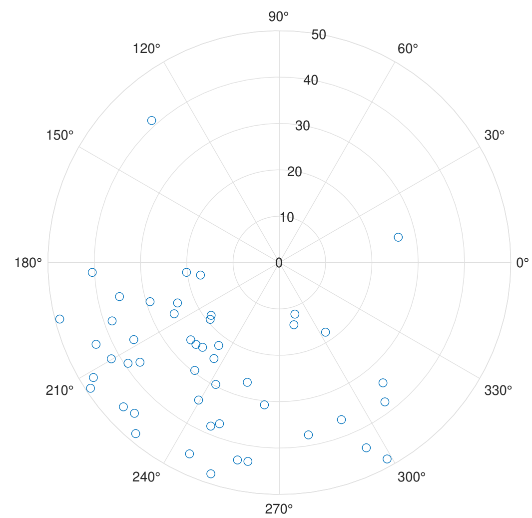

(a) Polar illustration.

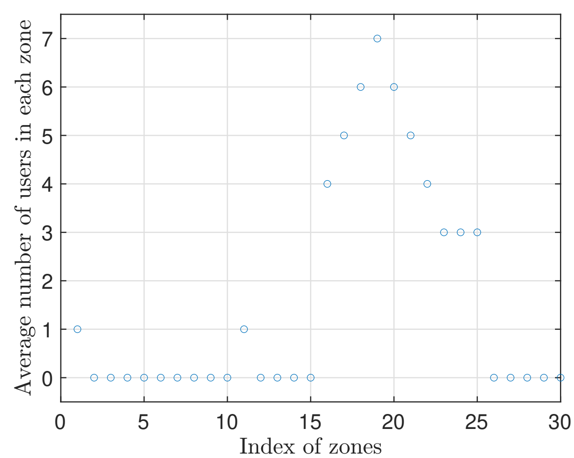

(b) Angular-domain illustration.

Fig. 5. User distribution-II.

the value of z_0 is necessary for achieving the maximum sum rate. For instance, when $B = 3$, $z_0 = 1$ needs to be selected to achieve the maximum sum rate. This is attributed to the rotational flexibility of the sector boundaries to achieve more favorable user distributions over sectors. In contrast, for user distribution-II, it is observed that there exists a performance gap between the maximum sum rate achieved by $B = 30$ versus that by other values of $B < 30$ (even under the optimal z_0), and the gap becomes more significant when B becomes smaller. This shows that the performance of the proposed flexible-sector BS is highly dependent on the underlying user distribution characteristics, in accordance with our analysis in Section VI-B. Therefore, it is imperative to tailor the flexible-sector BS parameters according to the specific user distributions for achieving the optimal performance.

Next, we compare the proposed flexible-sector BS design with other benchmark BS architectures in terms of the achievable sum rate for various total numbers of antennas N. To provide a comprehensive evaluation, we consider the following benchmarks:

- Antenna allocation only: The common rotation index is fixed with $z_0 = 1$. Accordingly, the antenna resources are flexibly allocated among sectors, i.e., N_b's are optimized based on Proposition 1.
- Sector rotation only: The number of antennas are equally allocated over sectors, i.e., $N_b = \frac{N}{B}, \forall b \in \mathcal{B}$. The common rotation index z_0 is optimized via the exhaustive search in Section V-B.
- Conventional fixed-sector architecture: Both the common rotation index z_0 and the antenna allocation are fixed, with $z_0 = 1$ and $N_b = \frac{N}{B}, \forall b \in \mathcal{B}$.

It is worth noting that, for the benchmark with sector rotation

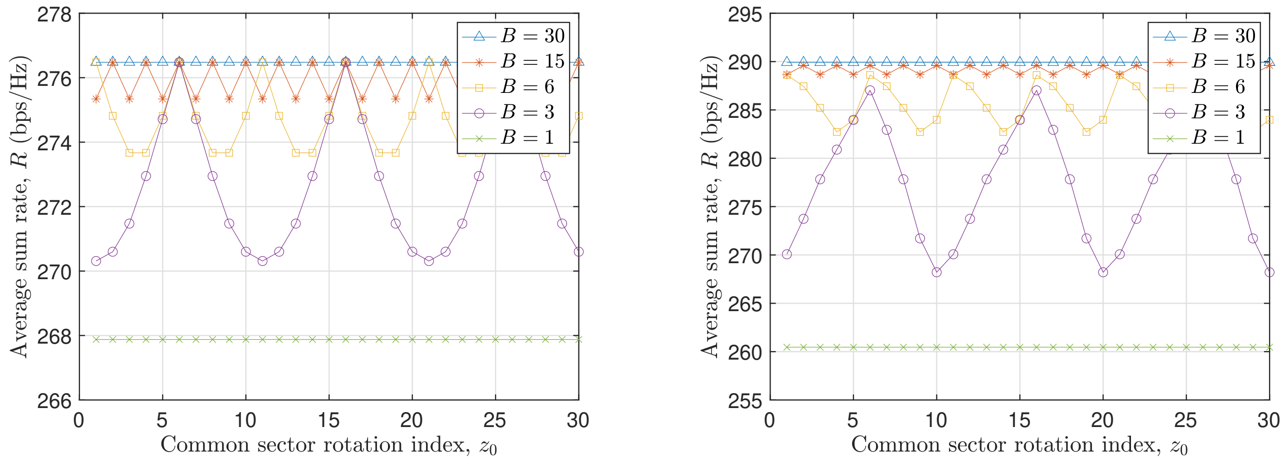

(a) User distribution-I.

(b) User distribution-II.

Fig. 6. Average sum rate versus z_0 under different user distributions.

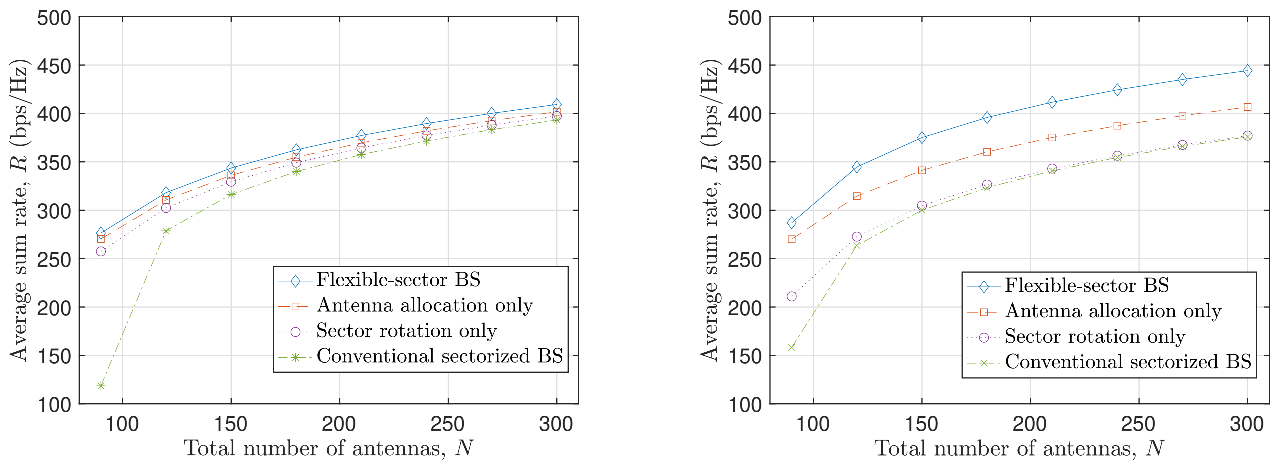

(a) User distribution-I.

(b) User distribution-II.

Fig. 7. Performance comparison of the flexible-sector BS with other benchmarks.

only, it is expected that the optimal performance is achieved when user distribution is as balanced as possible among the sectors to ensure equitable workload distribution and effective interference management, similarly as in the conventional cellular system design [37]. However, this is different from our proposed flexible-sector BS, which has the best sum rate under the opposite condition, i.e., when most users are located in one single sector, due to its antenna movement/reallocation capability (versus the fixed and equal antenna allocation in the case of sector rotation only).

Figs. 7(a) and 7(b) show the sum rate of all users versus the total number of antennas N under the two user distributions, respectively. It is observed that a larger value of N leads to performance improvements across all four BS architectures for both user distribution scenarios. Notably, the performance gain is more pronounced for user distribution-II, since it exhibits a relatively less uniform spatial distribution of users compared to user distribution-I, which is consistent with our analysis in Section VI-B. It is also observed that the proposed flexible-sector BS always achieves superior performance to other benchmark schemes. This consistent improvement is attributed to the increased adaptability of the flexible-sector BS design for sectors rotation and antenna allocations. Furthermore, the antenna allocation only scheme is observed to yield the second-best performance, and significantly outperforms the sector rotation only scheme, underscoring the significant role of optimal antenna allocation via antenna movement in matching the user spatial distribution. It is also shown that as the total number of antennas becomes sufficiently large, the performance gain provided by sector rotation diminishes, by comparing the two benchmarks, namely the sector rotation only and the conventional sectorized BS.

VIII. Conclusion

This paper proposes a novel flexible-sector BS architecture, which allows the common rotation of the sectors and dynamic antenna allocations among them to adapt to the spatial distribution of users. We develop an efficient two-step algorithm to obtain the solution of both common sector rotation and antenna allocations. It is shown that under given rotation, the optimal antenna allocation for each sector is a linear function with respect to the number of users in that sector. It is also shown that the proposed flexible-sector BS is particularly beneficial for scenarios with highly non-uniform, clustered user distributions. Numerical evaluations indicate that the proposed flexible-sector BS consistently outperforms benchmark schemes, owing to its superior ability to accommodate spatially varying user distributions. Collectively, these properties position the flexible-sector BS as a compelling architecture for future wireless networks, which are expected to exhibit heterogeneous user distributions, time-varying channel conditions, and diverse quality-of-service (QoS) requirements.

Appendix A
Proof of Lemma 1

It can be shown that given $a, b > 0$, $f(x) = \log_2(1+ax)$ is concave over $x > 0$, and $g(x) = \log_2(1+b/x)$ is convex over $x > 0$. As a result, according to the Jensen's inequality, $r_b^{(\mathrm{l})}$ given in (15) and $r_b^{(\mathrm{u})}$ given in (14) serve as the lower bound and upper bound of r_b, respectively [46].

Based on the orthogonal property of ZF combining, the combining vector $\boldsymbol{w}_k$ for user k in sector b is orthogonal to the subspace spanned by the channel vectors from the other Q_b-1 users in the same sector. Then, according to [47, Theorem 1.1], the upper bound $r_b^{(\mathrm{u})}$ given in (14) can be achieved, and the detailed proof is similar to that of [46, Theorem 2], and thus is omitted.

Let $\boldsymbol{G}_b = [\boldsymbol{g}_1, \cdots, \boldsymbol{g}_{Q_b}] \in \mathbb{C}^{Q_b \times N_b}$. Note that since the wireless channels between users and the BS follow the Rayleigh fading, i.e., $\boldsymbol{g}_k \sim \mathcal{CN}(\boldsymbol{0}, \boldsymbol{I}_{N_b})$, $(\boldsymbol{G}_b^H \boldsymbol{G}_b)^{-1}$ is a Wishart matrix [48]. According to [48, Lemma 2.10], we have

$$\mathbb{E}[\mathrm{tr}((\boldsymbol{G}_b^H \boldsymbol{G}_b)^{-1})] = \frac{Q_b}{N_b - Q_b}, \tag{49}$$

and

$$\mathbb{E}\left[[(\boldsymbol{H}_b^H \boldsymbol{H}_b)^{-1}]_{k,k}\right] = \frac{B}{N_b - Q_b}. \tag{50}$$

Therefore, the lower bound $r_b^{(\mathrm{l})}$ given in (15) can be achieved. This completes the proof.

Appendix B
Derivation of (25) and (26)

By applying the Lagrange multipliers to problem (P3), we obtain the Lagrangian of (P3) as

$$L(\boldsymbol{n}, \boldsymbol{\mu}, \nu) = \sum_{b=1}^{B} Q_b \log_2 \left[1 + B\gamma_0(N_b - Q_b)\right]$$
$$+ \boldsymbol{\mu}^T(\boldsymbol{n} - \boldsymbol{n}_{\min}) - \nu \left(\sum_{b=1}^{B} N_b - N\right), \tag{51}$$

where $\boldsymbol{n}_{\min} \triangleq \{N_{1,\min}, \cdots, N_{B,\min}\}$, $\boldsymbol{\mu} \triangleq \{\mu_1, \cdots, \mu_B\}$, $\nu \geq 0$, and $\mu_b \geq 0$ are the Lagrange multipliers associated with constraints (24a) and (24b) in problem (P3), respectively. Thus, by applying the Karush-Kuhn-Tucker (KKT) conditions, we have

$$N_b^\star \geq N_{b,\min}, \quad \forall b \in \mathcal{B}, \tag{52a}$$

$$N \geq \sum_{b=1}^{B} N_b^\star, \tag{52b}$$

$$0 = \left(\nu - \frac{Q_b}{\ln 2\left(N_b^\star - Q_b + \frac{1}{B\gamma_0}\right)}\right)(N_b^\star - N_{b,\min}), \forall b \in \mathcal{B}, \tag{52c}$$

$$\nu \geq \frac{Q_b}{\ln 2\left(N_b^\star - Q_b + \frac{1}{B\gamma_0}\right)}, \quad \forall b \in \mathcal{B}. \tag{52d}$$

Based on (52a)-(52d), we determine $N_b^\star$ in two cases:

- If $\mu_b > 0$ and
$$\nu \geq \frac{Q_b}{\ln 2}\left(N_{b,\min} - Q_b + \frac{1}{B\gamma_0}\right)^{-1}, \tag{53}$$
we have
$$N_b^\star = N_{b,\min}, \forall b \in \mathcal{B}. \tag{54}$$
- If $\mu_b = 0$ and
$$\nu < \frac{Q_b}{\ln 2}\left(N_{b,\min} - Q_b + \frac{1}{B\gamma_0}\right)^{-1}, \tag{55}$$
we have
$$N_b^\star = Q_b\left(1 + \frac{1}{\nu^\star \ln 2}\right) - \frac{1}{B\gamma_0}, \quad b \in \mathcal{B}. \tag{56}$$

Therefore, the solution for problem (P3) is given by (25).

Appendix C
Solution of Problem (P5)

By applying the Lagrange multiplier, we have

$$L(\boldsymbol{q}, \xi) = \sum_{b=1}^{B} Q_b \log_2(Q_b \eta) + \xi\left(\sum_{b=1}^{B} Q_b - K\right), \tag{57}$$

where $\eta = \frac{B\gamma_0(N-K+\frac{1}{\gamma_0})}{K}$, and ξ is the Lagrange multiplier associated with constraint (42a). Then, by solving the KKT conditions of (57) and mapping back to the discrete domain, we have

$$Q_b^\star = \left\lfloor 2^{-\xi - \frac{1}{\ln 2}} \frac{K}{B\gamma_0(N + \frac{1}{\gamma_0} - 1)} \right\rfloor, \quad \forall b \in \mathcal{B}. \tag{58}$$

As such, the optimal solution for problem (P5) corresponds to the case when the users are equally distributed among sectors.

References

[1] E. Telatar, "Capacity of multi-antenna Gaussian channels," *Eur. Trans. Telecommun.*, vol. 10, no. 6, pp. 585–595, Nov. 1999.

[2] R. W. Heath Jr and A. Lozano, *Foundations of MIMO communication*. Cambridge University Press, 2018.

[3] G. Stuber, J. Barry, S. McLaughlin, Y. Li, M. Ingram, and T. Pratt, "Broadband MIMO-OFDM wireless communications," *Proc. IEEE*, vol. 92, no. 2, pp. 271–294, Feb. 2004.

[4] A. J. Paulraj, D. A. Gore, R. U. Nabar, and H. Bolcskei, "An overview of MIMO communications-A key to gigabit wireless," *Proc. IEEE*, vol. 92, no. 2, pp. 198–218, Feb. 2004.

[5] L. Lu, G. Y. Li, A. L. Swindlehurst, A. Ashikhmin, and R. Zhang, "An overview of massive MIMO: Benefits and challenges," *IEEE J. Sel. Topics Signal Process.*, vol. 8, no. 5, pp. 742–758, Oct. 2014.

[6] S. A. Busari, K. M. S. Huq, S. Mumtaz, L. Dai, and J. Rodriguez, "Millimeter-wave massive MIMO communication for future wireless systems: A survey," *IEEE Commun. Sur. Tuts.*, vol. 20, no. 2, pp. 836–869, 2nd Quart. 2017.

[7] Z. Wan, Z. Gao, F. Gao, M. Di Renzo, and M.-S. Alouini, "Terahertz massive MIMO with holographic reconfigurable intelligent surfaces," *IEEE Trans. Commun.*, vol. 69, no. 7, pp. 4732–4750, Jul. 2021.

[8] T. L. Marzetta, "Massive MIMO: An introduction," *Bell Labs Tech. J.*, vol. 20, pp. 11–22, 2015.

[9] M. A. Albreem, M. Juntti, and S. Shahabuddin, "Massive MIMO detection techniques: A survey," *IEEE Commun. Surv. Tut.*, vol. 21, no. 4, pp. 3109–3132, 4th Quart. 2019.

[10] E. Björnson, L. Sanguinetti, H. Wymeersch, J. Hoydis, and T. L. Marzetta, "Massive MIMO is a reality—What is next?: Five promising research directions for antenna arrays," *Digit. Signal Process.*, vol. 94, pp. 3–20, Nov. 2019.

[11] E. G. Larsson, O. Edfors, F. Tufvesson, and T. L. Marzetta, "Massive MIMO for next generation wireless systems," *IEEE Commun. Mag.*, vol. 52, no. 2, pp. 186–195, Feb. 2014.

[12] H. Hua, T. X. Han, and J. Xu, "MIMO integrated sensing and communication: CRB-rate tradeoff," *IEEE Trans. Wireless Commun.*, vol. 23, no. 4, pp. 2839–2854, Aug. 2023.

[13] Z. Wang, J. Zhang, H. Du, D. Niyato, S. Cui, B. Ai, M. Debbah, K. B. Letaief, and H. V. Poor, "A tutorial on extremely large-scale MIMO for 6G: Fundamentals, signal processing, and applications," *IEEE Commun. Surv. Tuts.*, vol. 26, no. 3, pp. 1560–1605, Jan. 2024.

[14] H. Lu, Y. Zeng, C. You, Y. Han, J. Zhang, Z. Wang, Z. Dong, S. Jin, C.-X. Wang, T. Jiang *et al.*, "A tutorial on near-field XL-MIMO communications toward 6G," *IEEE Commun. Surv. Tuts.*, vol. 26, no. 4, pp. 2213–2257, Apr. 2024.

[15] H. Hua, J. Xu, and R. Zhang, "Near-field integrated sensing and communication with extremely large-scale antenna array," *IEEE Trans. Wireless Commun.*, Early Access, 2025.

[16] H. Lu and Y. Zeng, "Communicating with extremely large-scale array/surface: Unified modeling and performance analysis," *IEEE Trans. Wireless Commun.*, vol. 21, no. 6, pp. 4039–4053, Jun. 2021.

[17] Z. Gao, L. Dai, D. Mi, Z. Wang, M. A. Imran, and M. Z. Shakir, "Mmwave massive-MIMO-based wireless backhaul for the 5G ultra-dense network," *IEEE Wireless Commun.*, vol. 22, no. 5, pp. 13–21, Oct. 2015.

[18] Y. Zhang, X. Wu, and C. You, "Fast near-field beam training for extremely large-scale array," *IEEE Wireless Commun. Lett.*, vol. 11, no. 12, pp. 2625–2629, Dec. 2022.

[19] D. Gesbert, M. Kountouris, R. W. Heath, C.-B. Chae, and T. Salzer, "Shifting the MIMO paradigm," *IEEE Signal Process. Mag.*, vol. 24, no. 5, pp. 36–46, Sep. 2007.

[20] J. Duplicy, B. Badic, R. Balraj, R. Ghaffar, P. Horváth, F. Kaltenberger, R. Knopp, I. Z. Kovács, H. T. Nguyen, D. Tandur *et al.*, "MU-MIMO in LTE systems," *EURASIP J. Wireless Commun. Netw.*, vol. 2011, pp. 1–13, Mar. 2011.

[21] C. Zeng, J.-B. Wang, M. Xiao, C. Ding, Y. Chen, H. Yu, and J. Wang, "Task-oriented semantic communication over rate splitting enabled wireless control systems for URLLC services," *IEEE Trans. Commun.*, vol. 72, no. 2, pp. 722–739, Feb. 2023.

[22] B. Zheng, C. You, and R. Zhang, "Double-IRS assisted multi-user MIMO: Cooperative passive beamforming design," *IEEE Trans. Wireless Commun.*, vol. 20, no. 7, pp. 4513–4526, Jul. 2021.

[23] W. K. New, K.-K. Wong *et al.*, "A tutorial on fluid antenna system for 6G networks: Encompassing communication theory, optimization methods and hardware designs," *IEEE Commun. Surv. Tuts.*, vol. 27, no. 4, pp. 2325–2377, Aug. 2024.

[24] L. Zhu, W. Ma, W. Mei, Y. Zeng, Q. Wu, B. Ning, Z. Xiao, X. Shao, J. Zhang, and R. Zhang, "A tutorial on movable antennas for wireless networks," *IEEE Commun. Surv. Tuts.*, Early Access, 2025.

[25] L. Zhu, W. Ma, Z. Xiao, and R. Zhang, "Performance analysis and optimization for movable antenna aided wideband communications," *IEEE Trans. Wireless Commun.*, vol. 23, no. 12, pp. 18 653–18 668, Dec. 2024.

[26] Y. Chen, Z. Ren, X. Yu, L. Liu, and J. Xu, "Exploiting moving arrays for near-field sensing," *IEEE Wireless Commun. Lett.*, vol. 14, no. 3, pp. 601–605, Mar. 2025.

[27] W. Mei, X. Wei, B. Ning, Z. Chen, and R. Zhang, "Movable-antenna position optimization: A graph-based approach," *IEEE Wireless Commun. Lett.*, vol. 13, no. 7, pp. 1853–1857, Jul. 2024.

[28] S. Liu, X. Yu, J. Xu, and R. Zhang, "Near-field communication with massive movable antennas: A functional perspective," *arXiv preprint arXiv:2508.01201*, 2025.

[29] X. Shao, Q. Jiang, and R. Zhang, "6D movable antenna based on user distribution: Modeling and optimization," *IEEE Trans. Wireless Commun.*, vol. 24, no. 1, pp. 355–370, Jan. 2025.

[30] X. Shao, W. Mei, C. You, Q. Wu, B. Zheng, C.-X. Wang, J. Li, R. Zhang, R. Schober, L. Zhu *et al.*, "A tutorial on six-dimensional movable antenna for 6G networks: Synergizing positionable and rotatable antennas," *IEEE Commun. Surv. Tuts.*, Early Access, 2025.

[31] X. Shao, R. Zhang, Q. Jiang, and R. Schober, "6D movable antenna enhanced wireless network via discrete position and rotation optimization," *IEEE J. Sel. Areas Commun.*, Early Access, 2024.

[32] X. Shao and R. Zhang, "6DMA enhanced wireless network with flexible antenna position and rotation: Opportunities and challenges," *IEEE Commun. Mag.*, vol. 63, no. 4, pp. 121–128, 2025.

[33] X. Shao, R. Zhang, Q. Jiang, J. Park, T. Q. S. Quek, and R. Schober, "Distributed channel estimation and optimization for 6D movable antenna: Unveiling directional sparsity," *IEEE J. Sel. Top. Signal Process.*, vol. 19, no. 2, pp. 349–365, Mar. 2025.

[34] H. Hua, Y. Zhou, W. Mei, J. Xu, and R. Zhang, "Hierarchically tunable 6DMA for wireless communication and sensing: Modeling and performance optimization," *arXiv:2503.01317*, 2025.

[35] X. Shi, X. Shao, B. Zheng, and R. Zhang, "6DMA-aided cell-free massive MIMO communication," *IEEE Wireless Commun. Lett.*, vol. 14, no. 5, pp. 1361–1365, May. 2025.

[36] J. G. Andrews, S. Buzzi, W. Choi, S. V. Hanly, A. Lozano, A. C. K. Soong, and J. C. Zhang, "What will 5G be?" *IEEE J. Sel. Areas in Commun.*, vol. 32, no. 6, pp. 1065–1082, Jun. 2014.

[37] H.-N. Dai, K.-W. Ng, M. Li, and M.-Y. Wu, "An overview of using directional antennas in wireless networks," *Int. J. Commun. Syst*, vol. 26, no. 4, pp. 413–448, Apr. 2013.

[38] J. G. Andrews, A. K. Gupta, and H. S. Dhillon, "A primer on cellular network analysis using stochastic geometry," *arXiv:1604.03183*, 2016.

[39] M. Haenggi, *Stochastic Geometry for Wireless Networks*. Cambridge, U.K.: Cambridge Univ. Press, 2012.

[40] D. Stoyan, W. S. Kendal, and J. Mecke, *Stochastic geometry and its applications*. New York, NY, USA: Wiley, 1995, 1987, vol. 69.

[41] Y. Li and Y. J. Chun, "Analysis of IRS-assisted downlink wireless networks over generalized fading," *IEEE Trans. Wireless Commun.*, vol. 23, no. 8, pp. 10 182–10 197, Aug. 2024.

[42] Y. Li and Y. J. Chun, "Geometric view on integrated cascaded channel of IRS-aided communications," *IEEE Trans. Wireless Commun.*, vol. 23, no. 9, pp. 11 662–11 677, Sep. 2024.

[43] C. A. Balanis, *Antenna theory: analysis and design*. Hoboken, NJ, USA: Wiley, 2016.

[44] J. Lyu, Y. Zeng, and R. Zhang, "UAV-aided offloading for cellular hotspot," *IEEE Trans. Wireless Commun.*, vol. 17, no. 6, pp. 3988–4001, Jun. 2018.

[45] A. Goldsmith, *Wireless communications*. U.K.: Cambridge Univ., 2005.

[46] L. Liu, S. Zhang, and R. Zhang, "CoMP in the sky: UAV placement and movement optimization for multi-user communications," *IEEE Trans. Commun.*, vol. 67, no. 8, pp. 5645–5658, Aug. 2019.

[47] B. R. Marks and G. P. Wright, "A general inner approximation algorithm for nonconvex mathematical programs," *Oper. Res.*, vol. 26, no. 4, pp. 681–683, 1978.

[48] A. M. Tulino, S. Verdú *et al.*, "Random matrix theory and wireless communications," *Foundations and Trends® in Communications and Information Theory*, vol. 1, no. 1, pp. 1–182, 2004.